

Numerical methods based controller design for mobile robots

Gustavo Scaglia*, Lucía Quintero Montoya, Vicente Mut and Fernando di Sciascio

Instituto de Automática (INAUT), Universidad Nacional de San Juan, Av. Libertador San Martín 1109 (oeste), J5400ARL San Juan, Argentina.

(Received in Final Form: April 17, 2008. First published online: June 23, 2008)

SUMMARY

This paper presents the design of four controllers for a mobile robot such that the system may follow a preestablished trajectory. To reach this aim, the kinematic model of a mobile robot is approximated using numerical methods. Then, from such approximation, the control actions to get a minimal tracking error are calculated. Both simulation and experimental results on a PIONEER 2DX mobile robot are presented, showing a good performance of the four proposed mobile robot controllers. Also, an application of the proposed controllers to a leader robot following problem is shown; in it, the relative position between robots is obtained through a laser.

KEYWORDS: Nonlinear control; Trajectory control; Tracking; Mobile robots; Digital control; Numerical methods.

1. Introduction

One of the main problems found in mobile robot control is trajectory tracking. In general, the objective is that the mobile robot reaches the Cartesian position (x, y) with a preestablished orientation θ for each sampling period. These combined actions result in tracking the desired trajectory of the mobile robot. In order to achieve this objective, only two control variables are available: the linear velocity (V) and the angular velocity (W) of the robot (Fig. 1).

The use of path tracking in a navigation system is justified in structured workspaces as well as in partially structured workspaces where unexpected obstacles can be found during the navigation. In the first case, the reference trajectory can be set from a global trajectory planner. In the second case, the algorithms used to avoid obstacles replan the trajectory in order to avoid a collision; therefore, a new reference trajectory, which must be followed by the robot, is generated. Besides, there exist algorithms that express the reference trajectory of the mobile robot as function of a descriptor called r^1 or s (called *virtual time*)² whose derivative is function of the tracking error and the time t . For example, if the tracking error is large, the reference trajectory should wait for the mobile robot; on the other hand, if the tracking error is small, then the reference trajectory must tend to the original

trajectory calculated by the global planner. Accordingly, the module of trajectory tracking will use the original path or the online recalculated path as reference to obtain the smallest error when the mobile robot follows the path.³ Therefore, the path tracking is always important independently from whether the reference trajectory has been generated by a trajectory global planner or a trajectory local planner.

Several control strategies have been proposed for tracking trajectory, some of which are based on either the kinematic or the dynamic models of the mobile robot,^{4,5} depending on the operative speed and the precision of the dynamic model. Different structures to control these systems have been developed as well. In Tsuji *et al.*,⁶ the authors use a time-varying feedback gain whose evolution can be modified through the parameters that determine the convergence time and the behavior of the system. In the work of Fierro and Lewis,⁷ the controller proposed by Kanayama *et al.*⁸ is used. It generates the inputs to a velocity controller, making the position error asymptotically stable. Then, a controller to make the mobile robot velocity follow the reference velocity is designed. The work of Fukao *et al.*⁹ extends the design proposed by Kanayama *et al.*⁸ and considers that the model parameters are unknown. In the paper of Kim *et al.*,¹⁰ an adaptive controller which takes into account the parametric uncertainties and the robot external perturbations is proposed to guarantee perfect velocity tracking. The reference for velocity is obtained by using the controller proposed in 1990 by Kanayama *et al.*⁸ In Chwa,¹¹ two controllers have been designed. They are called position and heading controller. The former ensures the position tracking and the latter is activated when the tracking error is low enough and the tracking reference does not change its position. This reduces the error over the mobile robot orientation at the end of the path. In Shim and Sung,¹² the posture controller is designed depending on the posture error and in this way the reference velocities are generated based on a set of specifications such as (i) if the distance to a reference posture is large enough, then the movement is quick, and the speed is reduced as the robot approaches to the target; (ii) the robot should take less time to reach the desired posture. Later, the reference velocities go into a PID controller that generates the torque needed according to a desired speed.

In Sun and Cui,¹³ a controller for trajectory tracking is designed using the kinematic model of the mobile robot and a transformation matrix. Such matrix is singular if the linear velocity of the mobile robot is zero; therefore, the

* Corresponding author. E-mail: gscaglia@inaut.unsj.edu.ar

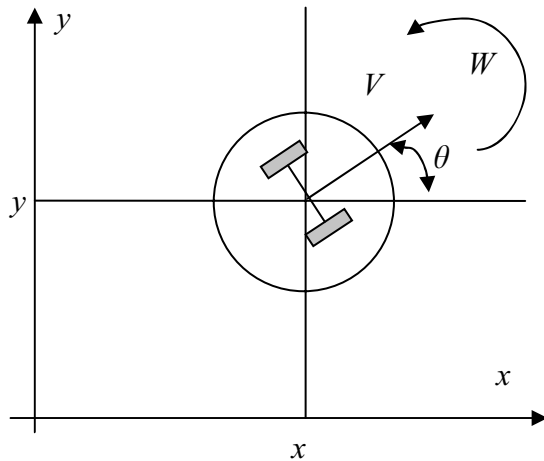


Fig. 1. Geometric description of the mobile robot.

effectiveness of this controller is only assured if the velocity is different from zero. Simulation results using linear velocity different from zero as initial condition are shown in this paper. In Sun,¹⁴ a controller based on the error model of Kanayama *et al.*⁸ is proposed. This controller is formed by two expressions, of which one or the other will be used depending on whether the angular velocity of the mobile robot is lower than a preestablished value ε or not.

In this work, the control scheme presented in Fierro and Lewis,⁷ Fukao *et al.*,⁹ Kim *et al.*,¹⁰ Shim and Sung,¹² and Cruz *et al.*¹⁵ will be used; first, a kinematic controller which generates the reference velocities to reach the desired goal is designed and second, the velocities obtained are used as input to the velocity controller. In our work a PID is used as a velocity controller, on board the PIONEER 2DX mobile robot, to maintain the robot's translational and rotational speeds at desired values, the same as in Shim and Sung¹² and Cruz *et al.*¹⁵ Besides, in our work it is not necessary to switch the controller as in Chwa¹¹ in cases when the position reference does not change and the tracking error is small. Our purpose is that when this situation is detected, the desired orientation changes, calculating the control signal by using the same expression.

In this paper, the designed controller does not present the disadvantage of the controller proposed by Sun and Cui,¹³ where a linear velocity different from zero is necessary. Furthermore, our controller does not need to change the control expression when the angular velocity is lower than a preestablished value.¹⁵

We propose to use numerical methods not only to simulate the evolution of the mobile robot, but also to find the control actions that allow going from the mobile robot current state to the next one. As a result, four controllers are obtained. Each one of these proposals is used according to the available information. Two of the obtained controllers make use of the velocity used to generate the reference and the other two do not need it. The main contribution of this work is that the four controllers are obtained by the same design methodology, and complex calculations to get the control signal are not necessary.

In this work, the simulation and experimental results are shown applied to a PIONEER 2DX mobile robot in which the error between the real and the desired trajectory is very small. The effectiveness and feasibility are then demonstrated in a practical sense through a set of experiments where the speed range is similar to the one reported in other papers about trajectory tracking using laboratory equipment, as in Normey-Rico *et al.*¹⁶

This paper is organized as follows: Section 2 presents the methodology to solve differential equations using numerical methods. Section 3 describes the kinematic model of the mobile robot approximated through numerical methods. In addition, the formulation of the proposed control algorithm is obtained. Section 4 presents the simulations and experimental results using the proposed controller on a PIONEER 2DX mobile robot and the redesign of the controller. In addition, the leader robot following problem in which the relative position of both robots is obtained through a laser sensor is considered. Finally, conclusions are detailed in Section 5.

2. Statement of the Problem

Let us consider the following differential equation:

$$\dot{y} = f(y, u, t); \quad y(0) = y_0 \quad (1)$$

where y represents the output of the system to be controlled, u the control action, and t the time. The values of $y(t)$ at discrete time $t = nT_0$, where T_0 is the sampling period, and $n \in \{0, 1, 2, 3, \dots\}$ will be denoted as y_n . Thus, when computing y_{n+1} by knowing y_n , Eq. (1) should be integrated over the time interval $nT_0 \leq t \leq (n+1)T_0$ as follows:

$$y_{n+1} = y_n + \int_{nT_0}^{(n+1)T_0} f(y, u, t) dt. \quad (2)$$

There are several numerical integration methods to calculate y_{n+1} . For instance, the Euler and trapezoidal method approaches can be used [Eqs. (3) and (4), respectively].

$$y_{n+1} \cong y_n + T_0 f(y_n, u_n, t_n) \quad (3)$$

$$y_{n+1} \cong y_n + \frac{T_0}{2} \{f(y_n, u_n, t_n) + f(y_{n+1}, u_{n+1}, t_{n+1})\} \quad (4)$$

where y_{n+1} on the right-hand side of Eq. (4) is not known and, therefore, can be estimated by Eq. (3). The use of numerical methods in the simulation of the system is based mainly on the possibility to determine the state of the system at instant $n+1$ from the state, the control action, and other variables at instant n . So, y_{n+1} can be substituted by the desired trajectory and then the control action to make the output system evolve from the current value (y_n) to the desired one can be calculated. To accomplish this, it is necessary to solve a system of linear equations for each sampling period, as shown in Section 3.

This work proposes applying this approximation to the kinematic model of a mobile robot and thus obtaining the control action that enables the robot to follow a preestablished

trajectory during its navigation. The next section will analyze the kinematic model of the mobile robot and the design of the proposed controller.

3. Methodology for Controller Design and Problem

Definition

A nonlinear kinematic model for a mobile robot will be used¹⁸ as shown in Fig. 1, represented by

$$\begin{cases} \dot{x} = V \cos \theta \\ \dot{y} = V \sin \theta \\ \dot{\theta} = W \end{cases} \quad (5)$$

where V is the linear velocity of the mobile robot, W is the angular velocity of the mobile robot, (x, y) is the Cartesian position, and θ is the orientation of the mobile robot. Then, the aim is to find the values of V and W so that the mobile robot may follow a preestablished trajectory. We assume that the mobile robot is moving on a horizontal plane without slip. In order to classify and develop our work properly, we made some considerations about the geometric conditions of the trajectory followed by the mobile robot.

First Hypothesis: $|\theta_{n+1} - \theta_n| < \lambda$, λ being a sufficiently small angle

Through the Euler's approximation of the kinematic model of the mobile robot [Eq. (5)], the following set of equations is obtained:

$$\begin{cases} x_{n+1} \approx x_n + T_0 V_n \cos \theta_n \\ y_{n+1} \approx y_n + T_0 V_n \sin \theta_n \\ \theta_{n+1} \approx \theta_n + T_0 W_n \end{cases} \quad (6)$$

This can be expressed in vectorial form as

$$\begin{bmatrix} x_{n+1} \\ y_{n+1} \\ \theta_{n+1} \end{bmatrix} = \begin{bmatrix} x_n \\ y_n \\ \theta_n \end{bmatrix} + T_0 \begin{bmatrix} \cos \theta_n & 0 \\ \sin \theta_n & 0 \\ 0 & 1 \end{bmatrix} \begin{bmatrix} V_n \\ W_n \end{bmatrix} \quad (7)$$

If the desired trajectory $[x_{d_{n+1}} y_{d_{n+1}} \theta_{d_{n+1}}]^T$ is known, then $[x_{n+1} y_{n+1} \theta_{n+1}]^T$ in Eq. (7) can be substituted by $[x_{d_{n+1}} y_{d_{n+1}} \theta_{d_{n+1}}]^T$ and thus it will be possible to calculate the control actions V_n, W_n necessary to make the mobile robot go from the current state $[x_n y_n \theta_n]^T$ to the desired one $[x_{d_{n+1}} y_{d_{n+1}} \theta_{d_{n+1}}]^T$. By defining

$$\begin{bmatrix} \Delta x \\ \Delta y \\ \Delta \theta \end{bmatrix} = \begin{bmatrix} x_{d_{n+1}} - x_n \\ y_{d_{n+1}} - y_n \\ \theta_{d_{n+1}} - \theta_n \end{bmatrix}, \quad B = \begin{bmatrix} \cos \theta_n & 0 \\ \sin \theta_n & 0 \\ 0 & 1 \end{bmatrix} \quad (8)$$

and then by replacing Eq. (8) into Eq. (7), the following equation is obtained:

$$B \begin{bmatrix} V_n \\ W_n \end{bmatrix} = \frac{1}{T_0} \begin{bmatrix} \Delta x \\ \Delta y \\ \Delta \theta \end{bmatrix} \quad (9)$$

Equation (9) is a system with three equations and two unknown variables, the optimal solution of which from mean squares is obtained from normal equation [Eq. (10)] (see ref. [19]).

$$B^T B \begin{bmatrix} V_n \\ W_n \end{bmatrix} = \frac{1}{T_0} B^T \begin{bmatrix} \Delta x \\ \Delta y \\ \Delta \theta \end{bmatrix} \Rightarrow B^T B = \begin{bmatrix} 1 & 0 \\ 0 & 1 \end{bmatrix};$$

$$B^T \begin{bmatrix} \Delta x \\ \Delta y \\ \Delta \theta \end{bmatrix} = \begin{bmatrix} \Delta x \cos \theta_n + \Delta y \sin \theta_n \\ \Delta \theta \end{bmatrix} \quad (10)$$

$$\begin{bmatrix} V_n \\ W_n \end{bmatrix} = \begin{bmatrix} \frac{\Delta x}{T_0} \cos \theta_n + \frac{\Delta y}{T_0} \sin \theta_n \\ \frac{\Delta \theta}{T_0} \end{bmatrix} \quad (11)$$

where V_n and W_n are the linear and angular velocities necessary to make the mobile robot go from the current state to the desired one.

To find a closed solution for the system of Eq. (9), it is necessary that real constants a_1 and a_2 exist such that

$$a_1 \begin{bmatrix} \cos \theta_n \\ \sin \theta_n \\ 0 \end{bmatrix} + a_2 \begin{bmatrix} 0 \\ 0 \\ 1 \end{bmatrix} = \begin{bmatrix} \Delta x \\ \Delta y \\ \Delta \theta \end{bmatrix}; \quad a_1, a_2 \in \Re \quad (12)$$

where

$$a_1 \begin{bmatrix} \cos \theta_n \\ \sin \theta_n \\ 0 \end{bmatrix} = \begin{bmatrix} \Delta x \\ \Delta y \\ 0 \end{bmatrix} \Rightarrow \frac{\sin \theta_n}{\cos \theta_n} = \frac{\Delta y}{\Delta x} \quad (13)$$

So, the desired orientation is defined by

$$\theta_{d_{n+1}} = a \tan \frac{y_{d_{n+1}} - y_n}{x_{d_{n+1}} - x_n} \quad (14)$$

where θ_d represents the necessary orientation to make the mobile robot tend to the reference trajectory. Then, the controller we propose for the mobile robot is given by

$$\begin{bmatrix} V_n \\ W_n \end{bmatrix} = \begin{bmatrix} kv \left(\frac{\Delta x}{T_0} \cos(\theta_{d_{n+1}}) + \frac{\Delta y}{T_0} \sin(\theta_{d_{n+1}}) \right) \\ kw \frac{\Delta \theta}{T_0} \end{bmatrix} \quad (15)$$

In Eq. (15), kv and kw are positive constants that allow us to adjust the performance of the proposed control system. They satisfy $0 < kv \leq 1$ and $0 < kw \leq 1$, allowing to reduce the variations in state variables as can be seen in Eqs. (16)–(19) and the explanation therein.

The next section will illustrate the simulation and experimental results of the control law obtained, under the assumption of the use of this controller over simple and nonexigent trajectories (in reference to the first hypothesis previously developed); then, the redesign of the controller, by using the same methodology, will be exposed in cases more complex than the first one and its performance on a mobile robot will show the feasibility of the method.

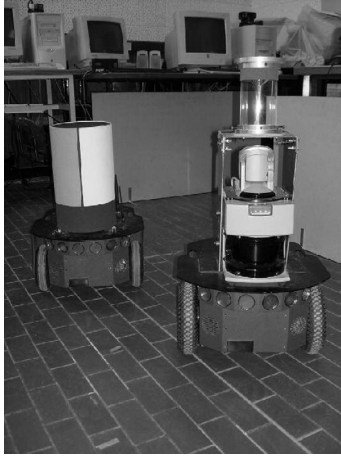


Fig. 2. PIONEER 2DX mobile robot and its environment.

4. Results, Discussion, and Controller Redesign

Simulation and experiments to test the proposed controller performance were carried out using a PIONEER 2DX mobile robot. The PIONEER 2DX mobile robot includes an estimation system based on odometry, which adds accumulative errors to the system. From this, updating the data through external sensors is necessary. This problem is separated from the strategy of trajectory tracking and it is not considered in this paper.^{3,16} The PIONEER 2DX has a PID velocity controller used to maintain the velocities of the mobile robot at the desired value (cf., refs. [12, 15]). Figure 2 shows the PIONEER 2DX and the laboratory facilities where the experiments were carried out. The simulation software SAPHIRA of Active Media was also used.²⁰

In order to test the performance of the proposed controller on a trajectory that satisfies the first hypothesis, a circumference of 600-mm radius was used as the desired one, with center on the origin of the coordinate system. The starting point for the robot was the center of the circumference, with an initial orientation $\theta = 0$ deg. From this starting point, it evolves to the desired trajectory. The

reference trajectory starts at (600, 0) mm and it is generated at constant linear and angular velocities, respectively known as V_{ref} and W_{ref} . In the PIONEER 2DX mobile robot, the value of the sample time T_0 is 0.1 s.

4.1. First approach (simulation and experimentation—index minimization)

A set of tests were developed in simulation and experimentation. A simulation using the SAPHIRA simulation software of Active Media²⁰ for the mobile robot was used, and the results are shown in Fig. 3(a) with $kv = kw = 1$ in Eq. (15), when V_{ref} is 100 mm/s. It can be noticed that the mobile robot follows the desired trajectory but in an oscillatory way. In order to correct this undesired behavior, the control actions can be calculated by the minimization of a quadratic index, in which not only the tracking error but also the square of state variables derivative has been considered, as seen in Eq. (16). Thus, the minimization of tracking error as well as the minimization of the variation of the state variables is considered

$$J = k_1^2 [(xd_{n+1} - x_{n+1})^2 + (yd_{n+1} - y_{n+1})^2] + k_2^2 \underbrace{(\dot{x}_n^2 + \dot{y}_n^2)}_{v_n^2} + k_3^2 (\theta_{d_{n+1}} - \theta_{n+1})^2 + k_4^2 \underbrace{\dot{\theta}_n}_{w_n^2} \quad (16)$$

We are looking for the derivative of the proposed index (16) with respect to the control actions to make a minimization. In (16), x_{n+1} , y_{n+1} , θ_{n+1} are given by Eq. (7). Next, working on Eq. (16) the following expressions can be reached:

$$\frac{\partial J}{\partial V_n} = k_1^2 [-2T_0 \cos \theta_n (xd_{n+1} - x_n - T_0 V_n \cos \theta_n) - 2T_0 \sin \theta_n (yd_{n+1} - y_n - T_0 V_n \sin \theta_n)] + k_2^2 2V_n = 0 \quad (17)$$

$$\frac{\partial J}{\partial W_n} = -2T_0 k_3^2 (\theta_{d_{n+1}} - \theta_n - T_0 W_n) + 2k_4^2 W_n = 0. \quad (18)$$

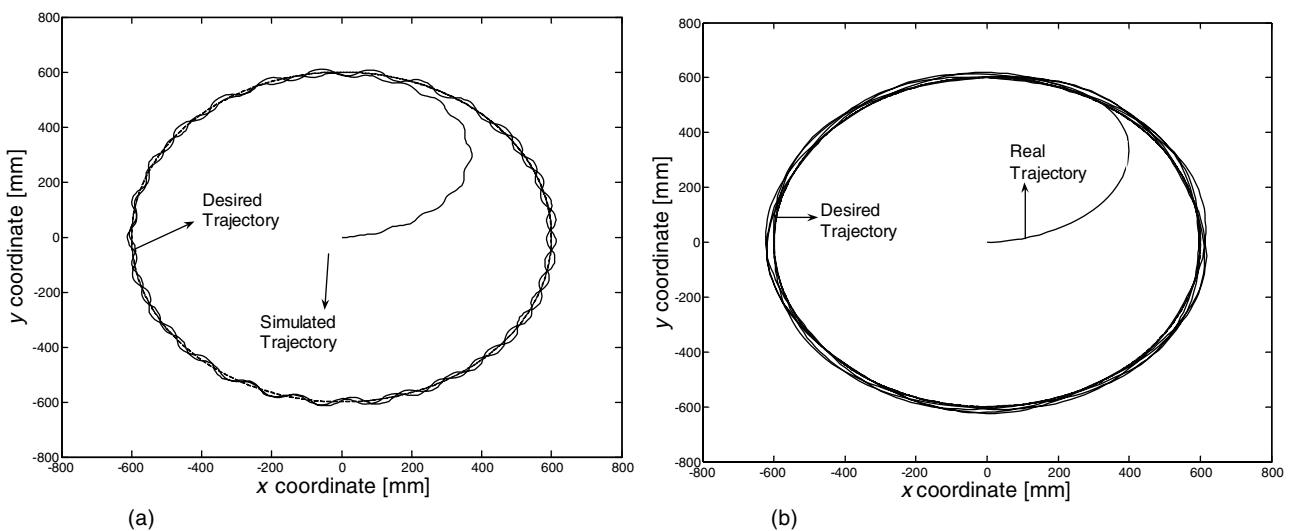


Fig. 3. (a) Simulation results: simulated and desired trajectory ($V_{ref} = 100$ mm/s, $kv = kw = 1$). (b) Experimental results: real and desired trajectory ($V_{ref} = 200$ mm/s, $W_{ref} = 19.1$ deg/s $kv = 0.2, kw = 0.2$).

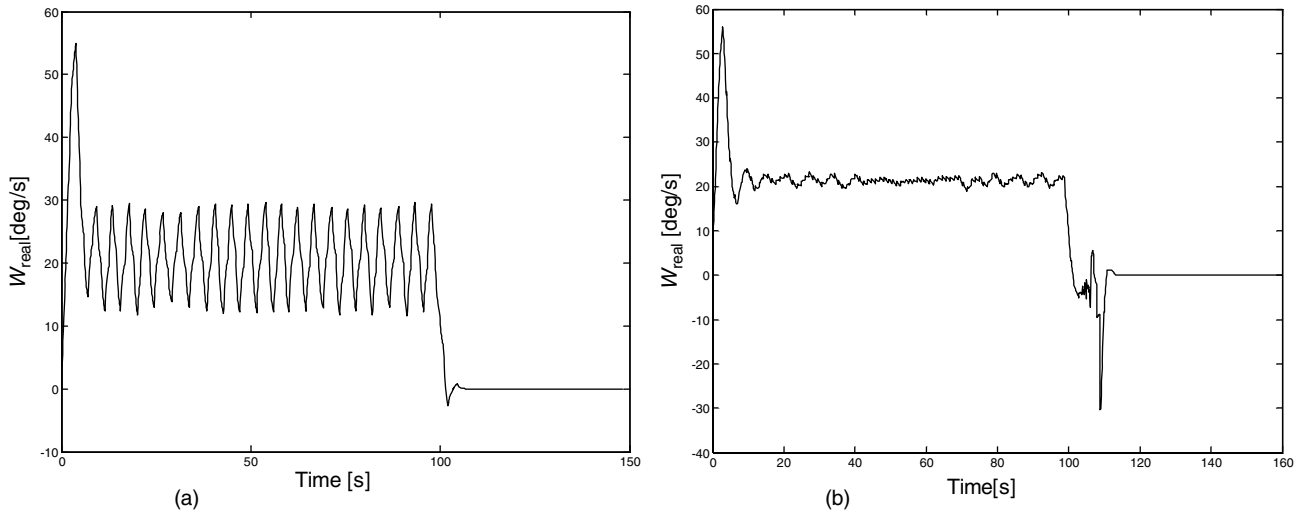


Fig. 4. Experimental results: (a) real angular velocity, controller Eq. (15). At $W_{ref} = 19.1$ deg/s; (b) real angular velocity, controller Eqs. (23) and (24). At $W_{ref} = 19.1$ deg/s.

From Eqs. (17) and (18), the expressions for the control actions V_n and W_n can be obtained:

$$\begin{cases} V_n = \frac{k_1^2}{k_1^2 + \frac{k_2^2}{T_0^2}} \left(\frac{\Delta x}{T_0} \cos \theta_n + \frac{\Delta y}{T_0} \sin \theta_n \right) \\ W_n = \frac{k_3^2}{k_3^2 + \frac{k_4^2}{T_0^2}} \frac{\Delta \theta}{T_0} \end{cases} \quad (19)$$

If Eqs. (15) and (19) are compared, then it can be seen that to minimize the state variables variations, the constant values of kv and k_w should be chosen to be less than 1; for that reason, we propose to reduce the values kv and k_w to values $kv = 0.2$ and $k_w = 0.2$. During the execution of the reference trajectory, at a random instant of time, certain values of (x_d, y_d) will be kept fixed. In this way, the proposed controller performance is monitored when a trajectory is to be followed by the mobile robot and then it is suddenly stopped at a certain point. From Fig. 3(b), experimental results on the mobile robot PIONEER 2DX can be analyzed, with $V_{ref} = 200$ mm/s and $W_{ref} = 19.1$ deg/s. Figure 3(b) shows the mobile robot following the reference trajectory without undesirable oscillations. The speed range used for testing the performance of the proposed controller is typical in the trajectory tracking papers referenced by the current bibliography.³ Figure 4(a) shows the time evolution of the real angular velocity, denoted as W_{real} , of the mobile robot.

It is important to remark that the absolute value of the difference between the desired and the real trajectory, once the mobile robot has reached the geometric predefined path, will be called *error*. In this way, Fig. 3(b) shows that the mobile robot follows the desired trajectory with a maximum error of 20 mm, which is very small compared to the distance between wheel axes (330 mm). However, linear and angular velocities present a considerable variation with respect to the reference value; it can be seen from Fig. 4(a) in reference to the angular velocity. To improve this issue, we propose

considering in index J the error between the current and desired state as well as the difference between the real and reference linear and angular velocities; this is

$$\begin{aligned} J = & cv1^2 \{ (xd_{n+1} - x_{n+1})^2 + (yd_{n+1} - y_{n+1})^2 \} \\ & + cw1^2 (\theta_{d_{n+1}} - \theta_{n+1})^2 + cv2^2 (V_{ref} - V_n)^2 \\ & + cw2^2 (W_{ref} - W_n)^2 + cv3^2 (\dot{x}_n^2 + \dot{y}_n^2) + cw3^2 \dot{\theta}_n \end{aligned} \quad (20)$$

where $cv1, cv2, cv3, cw1, cw2,$ and $cw3$ are constants that allow adjusting the control system response. By proceeding likewise,

$$\begin{aligned} \frac{\partial J}{\partial V_n} = 0 \Rightarrow V_n = & \frac{1}{cv1^2 + \frac{cv2^2}{T_0^2} + \frac{cv3^2}{T_0^2}} \\ & \times \left\{ cv1^2 \left[\frac{\Delta x}{T_0} \cos \theta_n + \frac{\Delta y}{T_0} \sin \theta_n \right] + \frac{cv2^2}{T_0^2} V_{ref} \right\} \end{aligned} \quad (21)$$

$$\begin{aligned} \frac{\partial J}{\partial W_n} = 0 \Rightarrow W_n = & \frac{1}{cw1^2 + \frac{cw2^2}{T_0^2} + \frac{cw3^2}{T_0^2}} \\ & \times \left\{ cw1^2 \frac{\Delta \theta}{T_0} + \frac{cw2^2}{T_0^2} W_{ref} \right\}. \end{aligned} \quad (22)$$

This can be expressed as

$$\begin{aligned} V_n = & \frac{kv^2}{kv1^2 + kv2^2} \left\{ kv1^2 \left[\frac{\Delta x}{T_0} \cos \theta_n + \frac{\Delta y}{T_0} \sin \theta_n \right] \right. \\ & \left. + kv2^2 V_{ref} \right\} \end{aligned} \quad (23)$$

$$W_n = \frac{k_w^2}{k_w1^2 + k_w2^2} \left\{ k_w1^2 \frac{\Delta \theta}{T_0} + k_w2^2 W_{ref} \right\} \quad (24)$$

Table I. Summary of the errors in the trajectory and the angular velocity for the experimental test by the use of controllers defined by Eqs. (19), (23), and (24).

V_{ref} (mm/s)	Maximum error controller by Eq. 19 (mm)	Maximum error controller by Eqs. 24 and 25 (mm)	Maximum angular speed difference for controller by Eq. 19 (deg/s)	Maximum angular speed difference for controller by Eqs. 24 and 25 (deg/s)
100	12	5	4.5	1.2
200	21	10	8	2
300	28	14	9.5	2.3

where $0 < kv^2 \leq 1$, $0 < kw^2 \leq 1$. Besides, it can be noticed that the control actions depend on the linear and angular reference velocities. To test the performance of the new control law obtained, another experiment was carried out using the values of $kv^2 = 1$, $kw^2 = 3.5$, $kw^2 = 1$, $kw^2 = 1.1$, $kw^2 = 0.22$, and $kv^2 = 0.24$ and the values of $V_{\text{ref}} = 200$ mm/s and $W_{\text{ref}} = 19.1$ deg/s. Figure 4(b) shows the time evolution of the angular velocity when the controller given by Eqs. (23) and (24) is used. The mobile robot follows the desired trajectory with a maximum error of 10 mm, which is very small considering the distance between the axes of the mobile robot (330 mm). It proves the good performance of the controller. In addition, if Figs. 4(a) and (b) are compared, it can be seen that the variation of the real angular velocity has been reduced considerably. A set of experiences was carried out at different reference velocities and a summary of these tests is presented in Table I; the most representative results of the experimental tests is shown in Fig. 4.

Another typical benchmark trajectory of reference, like a senoidal-type, was used to test the controller performance; in this case Fig. 5 shows the trajectory followed by the PIONEER 2DX mobile robot on the plane x - y , where the initial position of the mobile robot was $x = -4.0$ m, $y = 0$ m. It can be seen from Fig. 5 that the mobile robot tends to the desired trajectory and then follows it in a precise way. Figure 6(a) and (b) show the time evolution of the linear and angular velocities by using a PID controller to maintain the velocities on the reference values; Fig. 6(a) shows that the mobile robot goes at a high-linear-velocity compared with the speeds

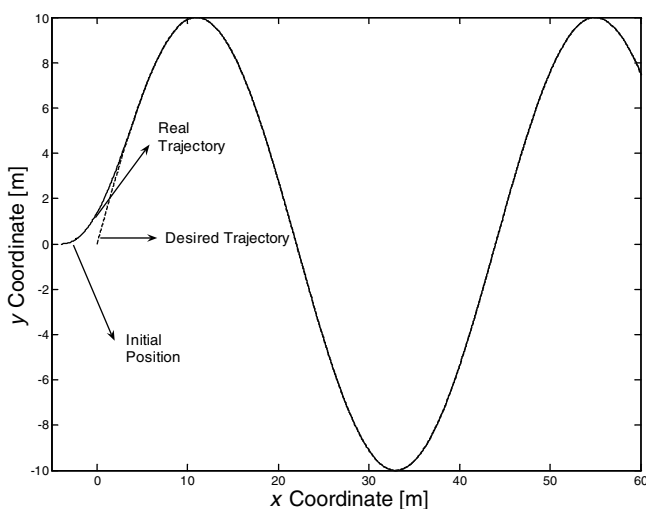


Fig. 5. Experimental results in lab facilities: real and desired trajectory.

commonly used in mobile robotics. In Fig. 6(b), we observe that the mobile robot is moving with a soft behavior without strong oscillations through the desired trajectory.

If a comparison between our experimental results and results recently published is made (for example Do and Pan,⁵ which presents an algorithm based on the dynamic model of the mobile robot showing simulation results), we conclude that the control system proposed in this paper presents a similar performance working at the same range of speeds. The maximum linear velocity was limited at 750 mm/s for safety conditions.

4.2. Second approach (trapezoidal-type integration method)

Second hypothesis: Value of $|\theta_{n+1} - \theta_n|$ higher than the one considered in the first hypothesis (It means the presence of sudden changes in the heading of the mobile robot along the desired trajectory).

Now, if Eq. (6) is not valid—a case occurring when the desired trajectory suddenly changes its direction—it is sensible to expect a momentarily increase of the error and then a decrease. To visualize these effects, a box of 2200 mm side is used as reference trajectory, which is generated at a constant linear speed ($V_{\text{ref}} = 200$ mm/s); the initial position of the mobile robot was $(-100, -100)$ mm. The experimental results are shown in Fig. 7(a) which displays the trajectory followed by the mobile robot PIONEER 2DX on the x - y plane. It can also be noticed that when the trajectory direction suddenly changes, the error increases, but it decreases afterwards, with a maximum error of about 100 mm. Besides, the error is not too large when compared with the size of the PIONEER 2DX, considering the demanding desired trajectory chosen. This trajectory-type is used to test the performance of the system, because it is a situation of *worst case*, where the error is acceptable since it is smaller than half the distance between the axes of the mobile robot. In other trajectory-types that satisfy the first hypothesis made, the performance will be better than in this case. However, a modification of the control algorithm is stated in order to reduce the peak in the trajectory shown in Fig. 7(a).

If in addition to knowing both the position and orientation of the mobile robot, the linear and angular velocities in nT_0 are also known, a trapezoidal-type integration approach can be made [see Eq. (4)]. In this way, another controller for a mobile robot is obtained and, consequently, it can be expected that the system behavior be enhanced due to the use of a better numerical approach of Eq. (5).

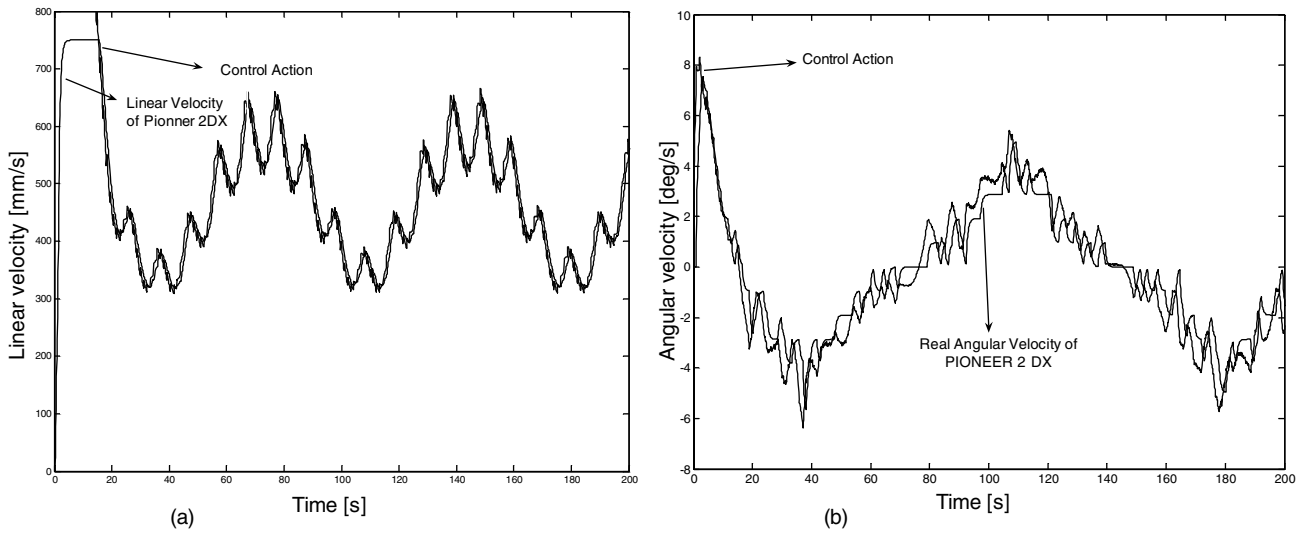


Fig. 6. Experimental results: (a) Control action [Eq. (23)] and real linear velocity of the mobile robot; (b) Control action [Eq. (24)] and real angular velocity of the mobile robot.

By the use of a trapezoidal-type integration method,

$$\begin{cases} x_{n+1} = x_n + \int_{nT_0}^{(n+1)T_0} V \cos \theta dt \approx x_n \\ \quad + \frac{T_0}{2} \{V_n \cos \theta_n + V_{n+1} \cos \theta_{n+1}\} \\ y_{n+1} = y_n + \int_{nT_0}^{(n+1)T_0} V \sin \theta dt \approx y_n \\ \quad + \frac{T_0}{2} \{V_n \sin \theta_n + V_{n+1} \sin \theta_{n+1}\} \\ \theta_{n+1} = \theta_n + \int_{nT_0}^{(n+1)T_0} W dt \approx \theta_n \\ \quad + \frac{T_0}{2} \{W_n + W_{n+1}\} \end{cases} \quad (25)$$

where x_n , y_n , θ_n , V_n , and W_n are the Cartesian position, orientation, linear velocity, and angular velocity at nT_0 , respectively. The aim is to find the values for θ_{n+1} , V_{n+1} , and W_{n+1} so that the mobile robot goes from its current

position (x_n, y_n) to $(x_{d_{n+1}}, y_{d_{n+1}})$. From Eq. (25),

$$\begin{cases} V_{n+1} \cos \theta_{n+1} = \frac{2}{T_0} (x_{d_{n+1}} - x_n) - V_n \cos \theta_n \\ V_{n+1} \sin \theta_{n+1} = \frac{2}{T_0} (y_{d_{n+1}} - y_n) - V_n \sin \theta_n \end{cases} \quad (26)$$

$$\frac{\sin \theta_{n+1}}{\cos \theta_{n+1}} = \tan \theta_{n+1} = \frac{\frac{2}{T_0} (y_{d_{n+1}} - y_n) - V_n \sin \theta_n}{\frac{2}{T_0} (x_{d_{n+1}} - x_n) - V_n \cos \theta_n}. \quad (27)$$

The value of θ_{n+1} is thus defined. As shown in Eq. (25), this is a three-equation system where linear and angular velocities are unknown; from Eq. (25),

$$\begin{bmatrix} \cos \theta_{n+1} & 0 \\ \sin \theta_{n+1} & 0 \\ 0 & 1 \end{bmatrix} \begin{bmatrix} V_{n+1} \\ W_{n+1} \end{bmatrix} = \begin{bmatrix} \frac{2}{T_0} (x_{d_{n+1}} - x_n) - V_n \cos \theta_n \\ \frac{2}{T_0} (y_{d_{n+1}} - y_n) - V_n \sin \theta_n \\ \frac{2}{T_0} \Delta \theta - W_n \end{bmatrix}. \quad (28)$$

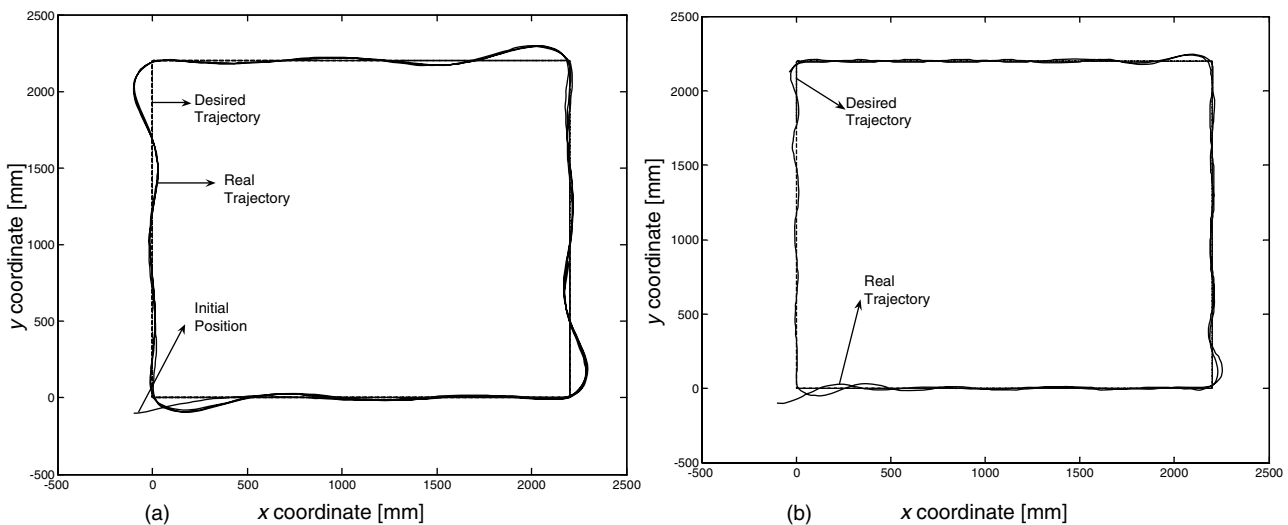


Fig. 7. Experimental results: (a) real and desired trajectory ($V_{ref} = 200$ mm/s). By using controller Eqs. (23) and (24). (b) Trajectory followed by the mobile robot on the x - y plane ($V_{ref} = 200$ mm/s). By using controller Eqs. (31) and (32).

And following the same steps in Eqs. (9) and (10), the following expression can be reached:

$$V_{n+1} = \frac{2}{T_0} \Delta x \cos \theta_{n+1} + \frac{2}{T_0} \Delta y \sin \theta_{n+1} - V_n \cos(\theta_{n+1} - \theta_n) \quad (29)$$

$$W_{n+1} = \frac{2}{T_0} \Delta \theta - W_n. \quad (30)$$

As in Eq. (15), the proposed controller will be defined by Eqs. (29) and (30), weighted with two constants. The aim of the modification to the original expression is to handle the controller influence over the system and improve its performance.

$$\begin{cases} V_{n+1} = kv \left[\frac{2}{T_0} \Delta x \cos \theta_{n+1} + \frac{2}{T_0} \Delta y \sin \theta_{n+1} - V_n \cos(\theta_{n+1} - \theta_n) \right] \\ W_{n+1} = kw \left[\frac{2}{T_0} \Delta \theta - W_n \right] \end{cases} \quad (31)$$

$$\tan \theta_{d_{n+1}} = \frac{\frac{2}{T_0} (y_{d_{n+1}} - y_n) - V_n \sin \theta_n}{\frac{2}{T_0} (x_{d_{n+1}} - x_n) - V_n \cos \theta_n} \quad (32)$$

where $0 < kv \leq 1$ and $0 < kw \leq 1$ allow reducing the oscillations in the state variables [see procedure in Eqs. (16)–(19)]. From Eqs. (31) and (32), we can observe that the control signals also depend on the current position, current orientation, and the linear and angular velocity of the mobile robot.

Figure 7(b) depicts an instance of the 2200-mm square-shaped reference trajectory followed by the PIONEER 2DX, generated with constant linear velocity of $V_{ref} = 200$ mm/s using the controller defined by Eqs. (31) and (32) from the robot's initial position of $(-100, -100)$ mm. If Figs. 7(a) and 7(b) both are compared, it can be seen that the performance of the controller improves. It means that the controller given

by Eq. (31) shows a better performance than that of the controller of Eqs. (23) and (24).

Figure 8(a) illustrates the trajectory followed by the PIONEER 2DX mobile robot on a plane x - y , when the reference velocity is $V_{ref} = 750$ mm/s using the controller defined by Eqs. (31) and (32), the used trajectory corresponds to the one defined by the first hypothesis. From this figure, it can be concluded that the value of error continues being small compared with the robot dimensions. This significant improvement, shown in Figs. 7(b) and 8(a), comes from using a better approximation of the system, which results in a controller which uses—in addition to the desired position and orientation—the real linear and angular velocities of the mobile robot. The speed range used to test the controller performance is typical in papers about trajectory tracking using laboratory equipment.^{16,17}

If the information about reference velocities is available, the previous control law can be modified by following the procedure indicated in Eqs. (20)–(24), thus, the linear and angular reference velocities are incorporated into the controller expressions as

$$\begin{cases} V_{n+1} = \frac{kv1^2}{kv1^2 + kv2^2} \left[kv1^2 \left(\frac{2}{T_0} \Delta x \cos \theta_{n+1} + \frac{2}{T_0} \Delta y \sin \theta_{n+1} - V_n \cos(\theta_{n+1} - \theta_n) \right) + kv2^2 V_{ref_{n+1}} \right] \\ W_{n+1} = \frac{kw1^2}{kw1^2 + kw2^2} \left[kw1^2 \left(\frac{2}{T_0} \Delta \theta - W_n \right) + kw2^2 W_{ref_{n+1}} \right] \end{cases} \quad (33)$$

The trajectory followed by the PIONEER 2DX mobile robot on the plane x - y , when the controller is described by Eq. (31) as well as Eq. (33), is shown in Fig. 8(a) and (b), respectively. A circumference with radio 600 mm and linear velocity of $V_{ref} = 750$ mm/s was used as reference trajectory.

Figure 8(a) and (b) shows that the error is very small for high velocities of the mobile robot. Nevertheless, comparing both control proposals, the performance obtained with the controller proposed by Eq. (33) is better than the one obtained

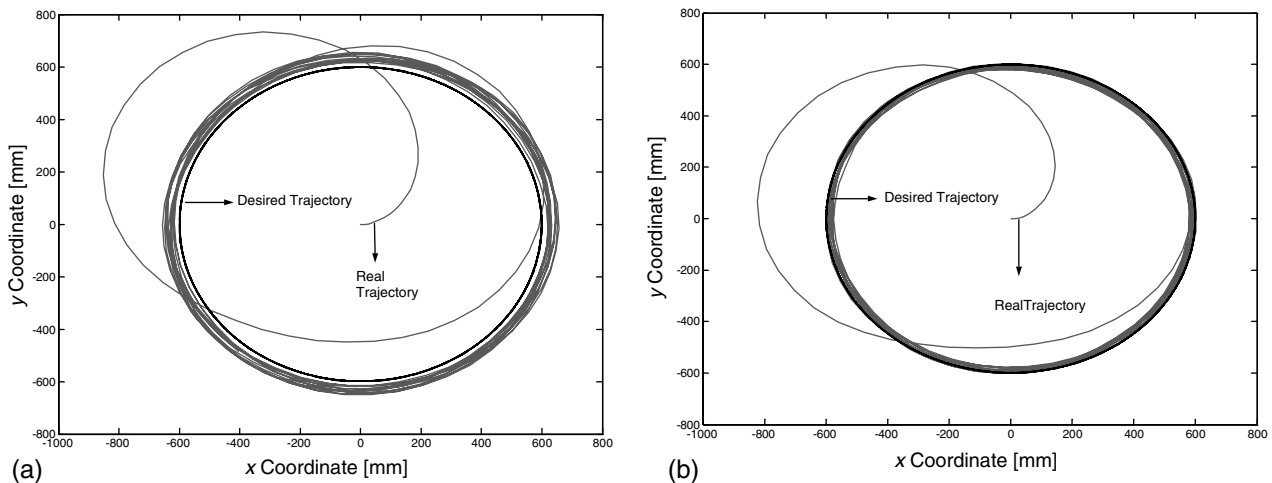


Fig. 8. Experimental results: Trajectory followed by the mobile robot on the x - y plane ($V_{ref} = 750$ mm/s): (a) Using controller defined by Eqs. (31) and (32); (b) Using controller defined by Eq. (33).

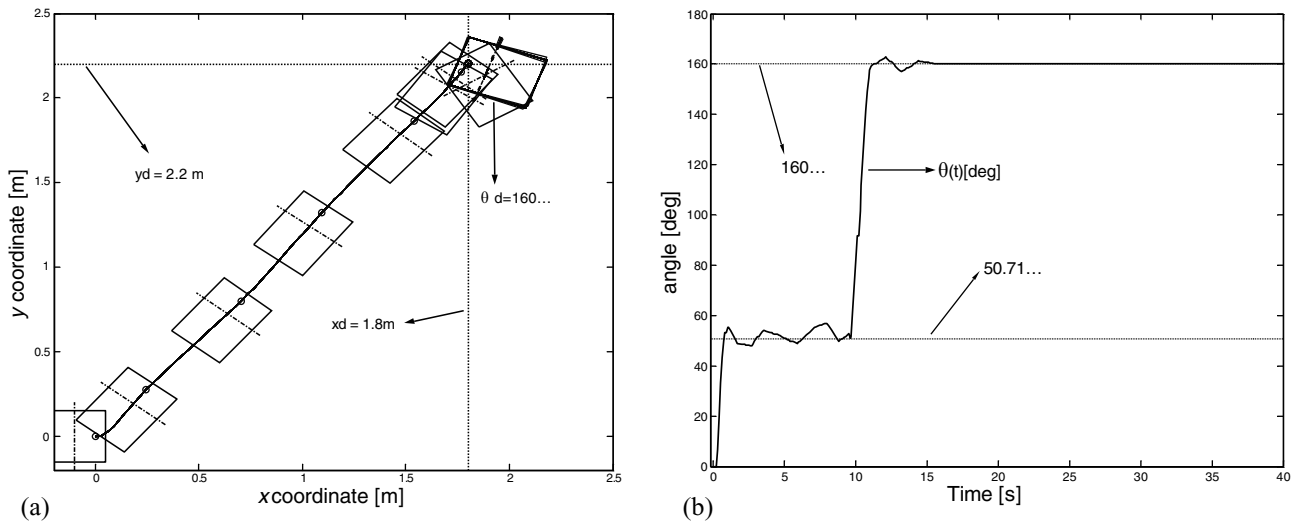


Fig. 9. Experimental results: (a) Trajectory followed by PIONEER 2DX in x - y plane; (b) time evolution of $\theta(t)$.

with the controller proposed by Eq. (31). This result is obtained since the controller proposed by Eq. (33) takes into account the reference velocities for the mobile robot, this is more information than the one in Eq. (31). It makes that the control action expressions use more information about the variables that influence the behavior of the robot.

4.3. Application examples (positioning and leader robot following)

Positioning: An important problem that has been previously studied¹¹ is the one in which the task is reaching a point in the plane x - y and then, making an orientation procedure with some desired angle of orientation established by a trajectory planner. Figure 9(a) shows the path followed by the mobile robot in plane x - y when the experiment considered was the problem of positioning. In that case, the values for the position and orientation were $xd = 1.8$ m, $yd = 2.2$ m, and $\theta d = 160$ deg. In Fig. 9(b), the orientation of the mobile robot depending on the time can be seen, where the initial values for position and orientation were $(x, y, \theta) = (0$ m, 0 m, 0 deg), respectively.

In case the positioning error is big, the orientation θd_{n+1} is calculated by using Eq. (32) and when the positioning error is small enough, it is assumed that $\theta d_{n+1} = 160$ deg. It means

$$\theta d_{n+1} = \begin{cases} a \tan \left(\frac{\frac{2}{T_0} (y d_{n+1} - y_n) - V_n \sin \theta_n}{\frac{2}{T_0} (x d_{n+1} - x_n) - V_n \cos \theta_n} \right) & \text{if } \sqrt{\Delta x^2 + \Delta y^2} > \varepsilon \\ 160 \text{ deg} & \text{if } \sqrt{\Delta x^2 + \Delta y^2} \leq \varepsilon \end{cases} \quad (34)$$

ε being a significantly small value, for this case, was used $\varepsilon = 0.01$ m. It can be seen from Fig. 9(a) and (b), how the mobile robot defines an orientation to reach the point $(x, y) = (1.8, 2.2)$ m and when it is close enough to its new desired orientation which is $\theta d_{n+1} = 160$ deg.

Leader robot following: Another example for the application of the proposed methodology is presented. In it,

the control objective is to make a robot follow a leader robot, keeping a predetermined distance. This tracking problem is solved through the use of the control laws obtained in Eqs. (31) and (32); since it is not necessary to use the linear and angular reference velocities in this example. Moreover, it can be clearly seen in this example that it does not exist dependency between the control scheme proposed and the odometry-based intern system. In leader robot following the relative position between both robots is obtained through an extern laser sensor.

In this section, the use of the developed controllers into a leader robot following problem is described. To reach this aim, a PIONEER 2DX mobile robot was used as a leader robot. From Fig. 10(a) the trajectory followed by both the leader robot and the follower robot in the plane x - y can be seen.

At the beginning of the trajectory, the leader advance was allowed until it reached a distance of 4 m from the follower; in that time, the advance of the follower robot was enabled. From Fig. 10(a) it can be observed that the follower robot quickly approaches the leader and then follows it with a distance of 0.28 m; the time evolution of the distance between both robots can be seen in Fig. 10(b). The relative position between both robots was obtained through a laser sensor.

An adequate and suitable performance of the proposed control system against a common robotics benchmark, like leader robot following, was shown in this example. Likewise, it can be observed that the proposed control system is dependent on the precision and accuracy of the sensor system, but independent from the sensor method used. This relies on the fact that not only intern sensors (odometry), but also extern sensors (laser) can be used depending on the application or the problem to solve.

5. Conclusions

In this work, four control laws have been proposed for the trajectory tracking of mobile robots. Each one of these controllers is used according to the available information. The first proposal is used only if the desired position is

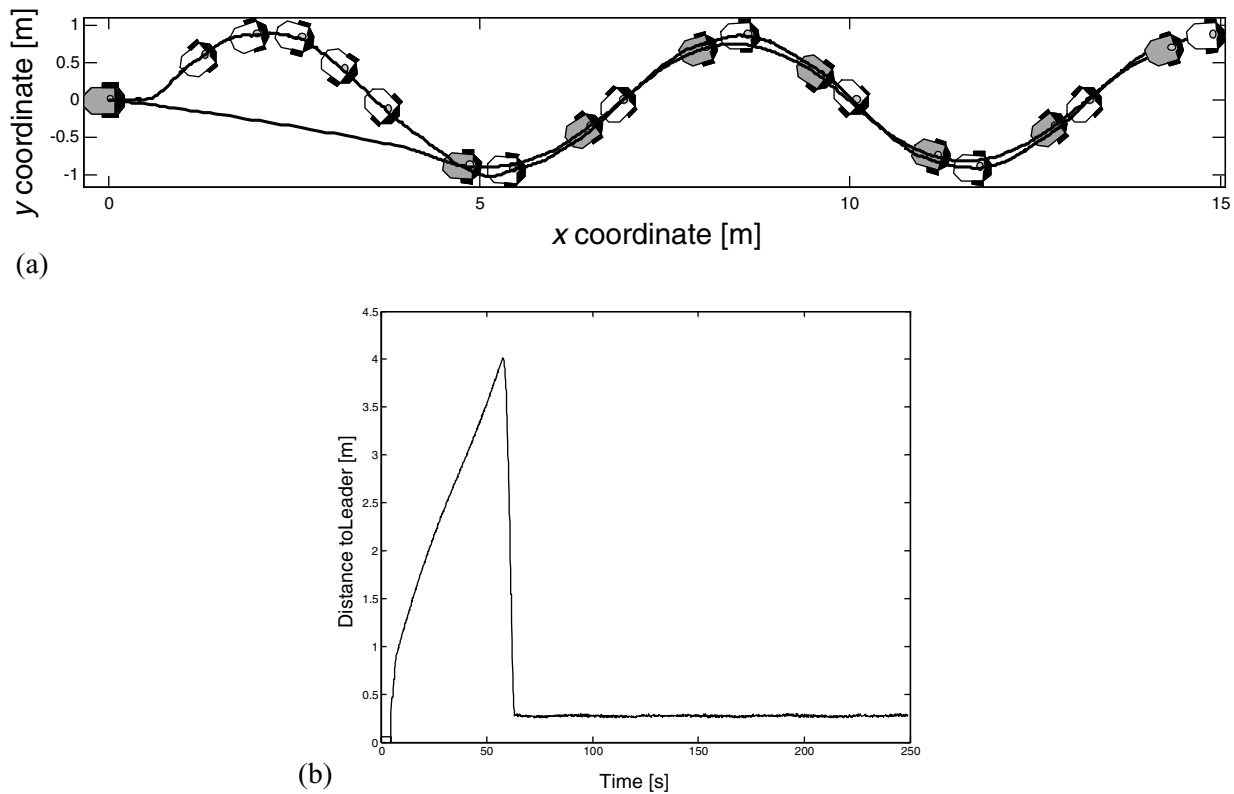


Fig. 10. Experimental results: (a) trajectory followed by robots in plane x - y ; (b) time evolution of the relative distance between both leader and follower robots.

available [Eq. (15)], the second one is applied when the desired position and desired velocity are available [Eqs. (23) and (24)], the third one is used when the position, orientation, linear velocity, and angular velocity are available [Eq. (31)], and finally, the fourth one is applied when the information used in the third one plus the linear and angular reference velocities are available [Eq. (334)]. The above control structures can be designed and implemented without great difficulty, because standard algebraic-numerical techniques are used.

Simulation and experimental results of the developed controllers on a PIONEER 2DX mobile robot have also been addressed. Through the analysis of these experiments, it can be concluded that the trajectory error between the desired and the real trajectories of the mobile robot is very small.

Also, the task of reaching a new reference point and then making a new orientation was considered. In this case, it can be seen that this goal was completely and efficiently reached without difficult calculations. Same results were obtained for the leader robot following problem exposed in this work.

From the experimental results, we conclude that the proposed methodology is quite simple for selecting the parameters of the controller in order to achieve a good performance of the system during the navigation of the mobile robot.

The proposed methodology for the controller design can be applied to other types of systems. The required precision of the proposed numerical method for the system approximation is smaller than the one needed to simulate the behavior of the system. This is because when the states for the feedback are available, in each sampling time, any difference from

accumulative errors is corrected (e.g., rounding errors). Thus, the approach is used to find the best way to go from one state to the next one, according to the availability of the system model. The controller design was also stated as a minimization of a quadratic index, which is a simple problem, and allows considering other trajectory properties, such as V_{ref} and W_{ref} .

Acknowledgments

This work was partially funded by the National Council of Scientific and Technological Research (CONICET), Argentina and the German Service for Academic Exchange (DAAD—Deutscher Akademischer Austausch Dients).

References

1. F. Del Rio, G. Jiménez, J. Sevillano, C. Amaya and A. Balcells, "Error Adaptive Tracking for Mobile Robots," *Proceedings of the 2002 28th Annual Conference of the IEEE Industrial Electronics Society*, Saville, Spain (2002) pp. 2415–2420.
2. S. Lee and J. H. Park, "Virtual Trajectory in Tracking Control of Mobile Robots," *Proceedings of the 2003 IEEE/ASME International Conference on Advanced Intelligent Mechatronic (AIM 2003)*, Port Island, Kobe, Japan (2003) pp. 35–39.
3. J. Normey-Rico, J. Gomez-Ortega and E. Camacho, "A Smith-predictor-based generalized predictive controller for mobile robot path-tracking," *Control Eng. Pract.* **7**, 729–740 (1999).
4. T. Lee, K. Song, C. Lee and C. Teng, "Tracking control of unicycle-modeled mobile robots using a saturation feedback controller," *IEEE Trans. Control Syst. Technol.* **9**(2) (Mar. 2001), pp. 305–318.

5. K. D. Do and J. Pan, "Global output-feedback path tracking of unicycle-type mobile robots," *Rob. Comput.-Integr. Manufact.*, **22**, 166–179 (2006).
6. T. Tsuji, P. Morasso and M. Kaneko, "Feedback Control of Nonholonomic Mobile Robots Using Time Base Generator," *Proceedings of IEEE International Conference on Robotics and Automation*, Nagoya Japan (1995), Vol. 2, pp. 1385–1390.
7. R. Fierro and F. Lewis, "Control of a Nonholonomic Mobile Robot: Backstepping Kinematics into Dynamics," *Proceedings of the 34th Conference on Decision & Control*, New Orleans, LA (Dec. 1995), Vol. 4, pp. 3805–3810.
8. Y. Kanayama, Y. Kimura, F. Miyazaki and T. Noguchi, "A Stable Tracking Control Method for an Autonomous Mobile Robot," *Proceedings of IEEE International Conference on Robotics and Automation*, Cincinnati, Ohio (1990) pp. 384–389.
9. T. Fukao, H. Nakagawa and N. Adachi, "Adaptive tracking control of a nonholonomic mobile robot," *IEEE Trans. Rob. Automat.* **16**(5) 609–615 (Oct. 2000).
10. S. Kim, J. Shin and J. Lee, "Design of a Robust Adaptive Controller for a Mobile Robot," *Proceedings of the 2000 IEEE/RSJ International Conference on Intelligent Robots and Systems*, Vol. 3, pp. 1816–1821.
11. D. Chwa, "Sliding-mode tracking control of nonholonomic wheeled mobile robots in polar coordinates," *IEEE Trans. Control Syst. Technol.* **12**(4) (July 2004).
12. H. Shim and Y. Sung, "Stability and four-posture control for nonholonomic mobile robots," *IEEE Trans. Rob. Automat.* **20**(1) (Feb. 2004).
13. S. Sun and P. Cui, "Path tracking and a practical point stabilization of mobile robot," *Rob. Comput.-Integr. Manufact.* **20**, 29–34 (2004).
14. S. Sun, "Designing approach on trajectory-tracking control of mobile robot," *Rob. Comput.-Integr. Manufact.* **21**(1), 81–85 (Feb. 2005).
15. D. Cruz, J. McClintock, B. Perteet, O. A. A. Orqueda, Y. Cao and R. Fierro, "Decentralized cooperative control—A multivehicle platform for research in networked embedded systems," *Control Syst. Mag. IEEE* **27**(3), 58–78 (June 2007).
16. J. Normey-Rico, I. Alcalá, J. Gomez-Ortega and E. Camacho, "Mobile robot path tracking using PID controller," *Control Eng. Pract.* **9**, 1209–1214 (2001).
17. W. Dixon, M. de Queiroz, D. Dawson and T. Flynn, "Adaptive tracking and regulation of a wheeled mobile robot with controller/update law modularity," *IEEE Trans. Control Syst. Technol.* **12**(1), 138–147 (Jan. 2004).
18. G. Campion, G. Bastin and B. d'Andrea-Novel, "Structural properties and classification of kinematic and dynamic models of wheeled mobile robots," *IEEE Trans. Rob. Automat.* **12**(1), 47–62 (Feb. 1996).
19. G. Strang, *Linear Algebra and Its Applications* (Academic Press, New York, 1980).
20. K. Konolige, "Saphira software manual version 6.1," Peterborough, NH-USA, ActivMedia Inc., October 1997.